Polyacrylamide crosslinked by bis-vinylimidazolium bromide for high elastic and stable hydrogels

Caihong Wang, [ID] Xiaoqin Guan, Yongli Yuan, Yong Wu [ID] and Shuai Tan [ID]*

A series of ionic compounds 1,*n*-dialkyl-3,3′-bis-l-vinylimidazolium bromide (C_nVIM) are prepared and employed to crosslink acrylamide for polyacrylamide (PAAM) hydrogel preparation *via in situ* solution polymerization. The swelling behavior, mechanical properties and thermal stability of the prepared C_nVIM crosslinked PAAM hydrogels are investigated. C_nVIM effectively crosslink the PAAM networks to form porous structures in the hydrogel, which could stably absorb water as much as 75.9 fold in weight without structural degradation. The prepared hydrogels could endure compressive stress up to 1.95 MPa and compressive deformation more than 90%. Meanwhile, the C_nVIM crosslinked networks show superior thermal stability, and could retain the structural integrity under 150 °C for more than 240 h. The swelling degradation resistance, mechanical strength and thermal stability of C_nVIM crosslinked hydrogels are much better than those of a conventional *N*,*N*′-methylenebisacrylamide crosslinked PAAM hydrogel. Using bis-vinylimidazolium bromides as crosslinkers provides an optional strategy for constructing thermally and mechanically robust hydrogel networks.

1 Introduction

Hydrogels, which are three-dimensional crosslinked hydrophilic networks absorbing large amounts of water, have attracted much attention due to their application in areas such as controlled drug delivery, tissue engineering, sensors, waste-water treatment and enhanced oil recovery.[1–7] In most cases, the applications of the hydrogels require considerable toughness to withstand mechanical loads and deformations. Although specially engineered hydrogels are known to exhibit excellent physical properties, they may suffer from drastic strength deterioration under some harsh conditions.[7–9] For example, the inevitable swelling of the hydrogel under different osmotic pressure would partly break the crosslinking networks, which greatly weaken the mechanical toughness of the hydrogels and limit the applicability in biological applications.[10] In the enhanced oil recovery fields, conventional polymer hydrogel systems are subject to fast thermal degradation for water management in high temperature petroleum reservoirs.[11,12] At present, developing tough hydrogels possessing sufficient mechanical strength under complex conditions remains a great challenge.

The crosslinking network plays a critical role for the stability of hydrogels, which leads researchers to seek suitable crosslinkers. Ionic liquids, which are defined as molten salts having melting points lower than 100 °C, have proved quite versatile for enabling a range of exciting applications due to their unique properties such as nonvolatility, high thermal stability and

friendly to environment.[13] Ionic liquids with divinyl moieties could be employed as crosslinker to copolymerized with monomers for polymer preparation.[14–16] For example, Gordon used an ionic liquid 1,8-di(vinylimidazolium)-octane bis[(trifluoromethyl)sulfonyl] amide to copolymerize with an ionic liquid monomer.[14] The prepared poly(ionic liquids) was thermally robust at temperatures up to 250 °C. Zhang *et al.* prepared superabsorbent polymers *via* copolymerization of acrylamide (AAM), acrylic acid and tetraallylammonium chloride.[15] The resulted crosslinking networks were thermally stable and could still absorb a large amount of water at 250 °C. In view of these, we envision that using ionic liquids as crosslinkers to construct hydrogel networks could improve the mechanical stability of the hydrogels to resist swelling and thermal degradation.

In this study, a series of ionic compounds 1,*n*-dialkyl-3,3′-bis-l-vinylimidazolium bromide (C_nVIM, *n* = 2, 6, 10) were prepared and utilized as crosslinkers for PAAM hydrogel preparation *via in situ* solution polymerization, as shown in Fig. 1. C_nVIM acted as effective crosslinkers in the copolymerization of hydrogels to form porous structures. Water swelling tests indicated that the C_nVIM crosslinked PAAM networks could stably absorb water up to 75.9 g g^{-1} to equilibrium. Compression tests suggested that C_nVIM crosslinked PAAM (C_nVIM–PAAM) hydrogel showed good mechanical strength and toughness under compression, which could withstand stresses higher than 1 MPa and compressive strains higher than 90% without fracture. Aging test revealed that C_nVIM–PAAM hydrogels possessed extraordinary thermal stability, which could tolerate 150 °C for more than 240 h with structural integrity. The swelling behavior, mechanical strength and thermal stability of C_nVIM–PAAM

School of Chemical Engineering, Sichuan University, No. 24 South Section 1, Yihuan Road, Chengdu 610065, China. E-mail: tanshuai@scu.edu.cn

Fig. 1 Schematic diagram of C$_n$VIM–PAAM hydrogel preparation and image of the resultant hydrogel.

hydrogel were much better than those of a *N,N′*-methyl-enebisacrylamide (MBA) crosslinked PAAM hydrogel.

2 Experimental

2.1 Materials

All commercially-available starting materials, reagents and solvents were obtained from TCI and Acros and used as supplied.

2.2 Characterization

The ^{1}H NMR spectra were obtained in D$_2$O using a Bruker AV II-400 spectrometer. The Fourier transform IR spectra were measured with the use of a Perkin Elmer Spectrum Two Li10014 spectrometer. Before measurements, C$_n$VIM–PAAM were freeze-dried under vacuum to constant weight in a Christ Alpha 1-2LD vacuum freeze dryer to remove the water. The scanning electron microscope (SEM) observations of the freeze-dried hydrogel samples were performed by a Nova NanoSEM 450 field emission SEM at an accelerating voltage of 5 kV. The thermogravimetric (TG) analyses of the freeze-dried hydrogel samples were conducted on a TA Q600 gravimetric analyzer over a temperature range of 30–600 °C at a heating rate of 10 °C min^{-1} under nitrogen atmosphere. Dynamic mechanical analysis (DMA) was performed on a TA Q800 dynamic mechanical analyzer. The samples for DMA measurements were prepared in the form of cylinder (35 mm in diameter and 4 mm in height). The sample were first subjected to a strain sweep test at constant frequency (1 Hz) in which they were deformed at different compress strains, and the modulus Ge was recorded to define the linear viscoelastic region in which the modulus is independent of the strain. 1% deformation was chosen to ensure that each measurement was made in linear viscoelastic region in frequency sweep tests (from 0.1 to 10 Hz at 25 °C). The compression tests were performed using an Instron 5967 electronic universal test machine at room temperatures. The compression tests of the samples (10 mm in diameter and 10 mm in height) were performed with a crosshead speed of 5 mm min^{-1}. Compressive modulus was calculated from the slope of the linear region of the stress–strain curve during the compression tests (strain: 10–15%). The fracture stress of the samples was defined as the stress at the breaking point.

2.3 Synthesis of 1,*n*-dialkyl-3,3′-bis-l-vinylimidazolium bromide (C$_n$VIM)

All the bis-vinylimidazolium bromide crosslinkers were prepared by procedures analogous to that described below for

C$_6$VIM. 1,6-Dibromohexane (3 ml, 10 mmol) and 1-vinyl-imidazole (2 ml, 22 mmol) were dissolved in methanol (5 mL). The mixture was stirred at 60 °C for 30 h, then ethyl acetate (50 ml) was added to precipitate resultant bis-vinylimidazolium bromide salt. The precipitate was separated through filtration, washed with ethyl acetate for twice and dried under vacuum to constant weight at 40 °C to give C$_6$VIM (4.1 g). Yield: 95%. ^{1}H NMR (400 MHz, D$_2$O, δ): 8.24, 7.94 (d, 4H, N–CH–CH–N), 7.36 (m, 2H, CH$_2$–CH–N), 5.69, 5.31 (m, 4H, CH$_2$=CH–N), 4.17 (t, 4H, CH$_2$–CH$_2$–N), 1.75 (t, 4H, CH$_2$–CH$_2$–N), 1.24 (t, 4H, CH$_2$–CH$_2$–CH$_2$–N); IR (KBr): ν = 3450, 3137, 3075, 2931, 2845, 1646, 1547, 1453, 1378, 1310, 1169, 1105, 957, 919, 830, 741, 630, 597 cm^{-1}; anal. calcd for C$_{16}$H$_{24}$Br$_2$N$_4$: C 44.46, H 5.60, N 12.96; found: C 44.40, H 5.58, N 12.9.

2.4 Synthesis of PAAM hydrogels

The C$_n$VIM–PAAM hydrogels were prepared by procedures analogous to that described below for C$_6$VIM–PAAM. The mole ratio of the crosslinker C$_n$VIM to the monomer AAM was controlled at 1 : 220. The composition of gelant solution for PAAM hydrogel preparation are listed in Table 1. C$_6$VIM (0.28 g, 0.64 mmol), AAM (10 g, 140.8 mmol) and ammonium persulfate (APS, 0.04 g, 0.18 mmol) were dissolved in deionized water (90 mL). The mixture was stirred at room temperature for 30 min for total dispersion. The gelant solution were sealed in a plastic mold and the polymerization of the gelant solution was carried out at 60 °C for 6 h. The resultant hydrogels were colorless and transparent, as shown in Fig. 1. IR (KBr): ν = 3450, 2935, 1668, 1458, 1420, 1343, 1126, 651 cm^{-1}.

A MBA crosslinked PAAM hydrogel (MBA–PAAM) was also prepared as a reference by procedures analogous to C$_n$VIM–PAAM preparation. The mole ratio of BIS to acrylamide was also controlled at 1 : 220.

3 Results and discussion

3.1 Hydrogel preparation

The successful preparation of the ionic crosslinkers C$_n$VIM and the C$_n$VIM–PAAM hydrogel were confirmed by ^{1}H NMR and IR spectra, as shown in Fig. 2. In the IR spectrum of AAM, the bands at 988 cm^{-1} and 962 cm^{-1} were ascribed to the bending vibration of the acryl bond. These bands disappeared in the spectrum of the freeze-dried C$_6$VIM–PAAM and a new band at 2935 cm^{-1} (the C–H stretching vibration in PAAM main chains) appeared in the spectrum of the freeze-dried C$_6$VIM–PAAM, which suggested the successful polymerization of AAM. The

Table 1 The composition of gelant solution for PAAM hydrogel preparation

Hydrogel	C_2VIM (g)	C_6VIM (g)	$C_{10}VIM$ (g)	MBA (g)	AAM (g)	APS (g)	H_2O (g)
C_2VIM–PAAM	0.24	—	—	—	10	0.04	90
C_6VIM–PAAM	—	0.28	—	—	10	0.04	90
$C_{10}VIM$–PAAM	—	—	0.32	—	10	0.04	90
MBA–PAAM	—	—	—	0.1	10	0.04	90
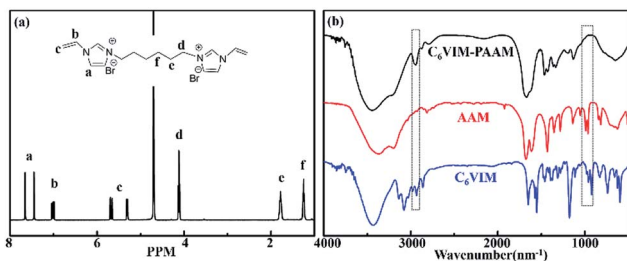
Fig. 2 (a) ^{1}H NMR spectrum of C_6VIM in D_2O; (b) IR spectra of C_6VIM, AAM and dried C_6VIM–PAAM.

bands at 3450 cm^{-1}, 1668 cm^{-1}, 1458 cm^{-1}, 1420 cm^{-1}, 1343 cm^{-1}, 1126 and 651 cm^{-1} in the FT-IR spectrum of the freeze-dried C_6VIM–PAAM were ascribed to the N–H stretching vibration, the C–H stretching vibration in the C=O stretching vibration of the amide group, the CH_2 scissoring vibration, the C–N stretching vibration of the amide group, the NH_2 scissoring vibration, the N–H in-plane vibration and the N–H out-of-plane vibration, respectively.[17] The FT-IR spectra of freeze-dried C_nVIM–PAAM were substantially identical to that of freeze-dried C_6VIM–PAAM.

The microstructures of the prepared C_nVIM–PAAM hydrogels were characterized by SEM analysis. The SEM images of freeze-dried C_nVIM–PAAM hydrogels were shown in Fig. 3. Honeycomb-like structure formed in the C_nVIM–PAAM hydrogels, indicating the successful formation of crosslinking networks. The average pore size of C_nVIM–PAAM was about 10 μm.
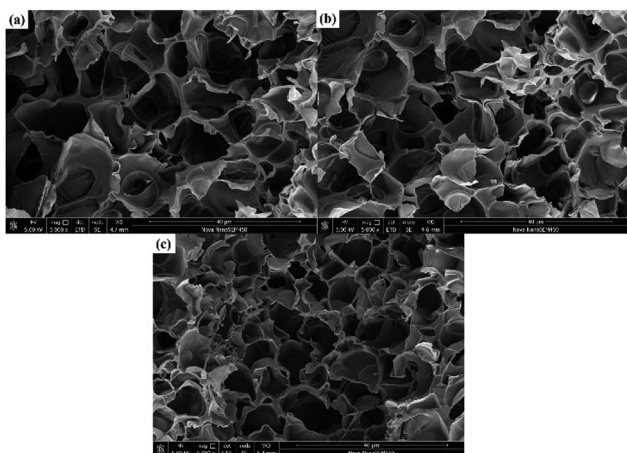
Fig. 3 SEM images of (a) freeze-dried C_2VIM–PAAM, (b) C_6VIM–PAAM, (c) $C_{10}VIM$–PAAM.

3.2 Swelling behavior

The water swelling behavior of the hydrogels was determined using a gravimetric method at room temperature. Before measurements, all the as-prepared hydrogels were shaped in same size. The samples were immersed into the deionized water and weighted at specific time until they reached swelling equilibrium to determine the water swelling ratio. Afterwards, the hydrogels were dried in a vacuum oven at 60 °C to constant weight. The water swelling ratio (SR) and equilibrium water content (EWC) of the hydrogels were calculated using the following equations:

$$SR = \frac{W_s}{W_o} \tag{1}$$

$$EWC = \frac{W_{sE} - W_d}{W_d} \tag{2}$$

where W_o, W_s, W_{sE} and W_d stand for the weights of the as-prepared hydrogel, the swollen hydrogel, the equilibrium swollen hydrogel and the totally dried hydrogel. The obtained swelling behavior of the hydrogels are shown in Fig. 4.

As shown in Fig. 4a, the swelling ratio of the C_nVIM–PAAM hydrogels grew rapidly in the initial 40 h and reached a steady state after about 120 h. The swelling ratio and the calculated equilibrium water content (inset of Fig. 4a) of C_nVIM–PAAM hydrogels increased with the length of the flexible alkyl chain in C_nVIM. The C_nVIM with longer flexible alkyl chain might form more loose crosslinking network to absorb more water. The equilibrium water content of the $C_{10}VIM$ crosslinked PAAM networks could reached up to 75.9 g g^{-1}. The C_nVIM crosslinked PAAM networks were robust to resist water swelling degradation. In spite of a high water content after equilibrium swelling, the equilibrium C_nVIM–PAAM hydrogels almost retained its
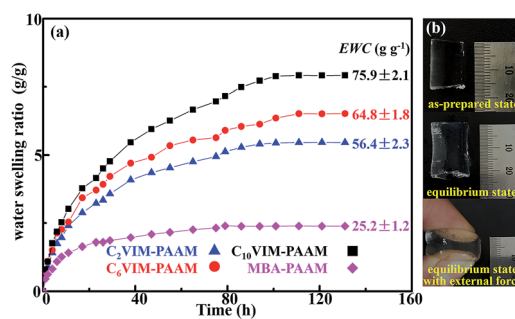
Fig. 4 (a) SR and EWC of the hydrogels as a function of time; (b) images of C_6VIM–PAAM hydrogel under as-prepared state and equilibrium state.

original volume and shape, and could still withstand external force (Fig. 4b). This result indicated "noneswellable" properties of C_nVIM–PAAM hydrogels, which was important for hydrogel application.[8,18] The C_nVIM–PAAM hydrogels swelled water faster and exhibited higher swelling ratio than the MBA–PAAM hydrogel, probably due to the strong hydrophilicity of the imidazolium moieties in the hydrogel networks.

3.3 Mechanical property

The viscoelastic properties of the C_nVIM–PAAM hydrogels were revealed by DMA tests. The measured elastic modulus of the as-prepared hydrogels as a function of frequency are shown in Fig. 5. For all the hydrogels, the storage modulus was always much higher than the loss modulus over the entire frequency range, which indicated that C_nVIM–PAAM formed a stable three-dimensional network.[19] The storage modulus of C_nVIM–PAAM increased slightly with the increase in shear frequency, which was a consequence of the viscoelastic nature of the hydrogel.[20] The flexible alkyl spacer in the crosslinker would reduce the rigidity of the crosslinking network in the hydrogels. As a result, the storage modulus of C_nVIM–PAAM decreased with the elongation of the alkyl chain in the crosslinker. All the C_nVIM–PAAM hydrogels exhibited plateau storage modulus higher than 30 kPa (35.0 ± 0.6 kPa for C_2VIM–PAAM, 33.8 ± 0.4 kPa for C_6VIM–PAAM and 30.8 ± 0.7 kPa for C_{10}VIM–PAAM), which was higher than previously reported PAAM hydrogels.[21–23] This result indicated the good viscoelastic property of the C_nVIM crosslinked networks. The storage modulus of C_nVIM–PAAM was also slightly higher than that of MBA–PAAM hydrogel, which might be ascribed to the rigid imidazolium moieties in the crosslinked networks.

The mechanical properties of the C_nVIM–PAAM hydrogels were revealed by uniaxial compressive tests. Compressive stress–strain curves of the hydrogels at a crosshead speed of 5 mm min^{-1} are shown in Fig. 6a. For C_nVIM–PAAM, the compressive stress gradually increased with the increase in strain till the strain reached about 70%. After that, the stress suddenly increased sharply. All the C_nVIM–PAAM hydrogels could withstand a compressive deformation of 90% strain and a compress stress of 1 MPa without facture, which revealed good mechanical strength and toughness of the hydrogels. The compressive modulus, the fracture stress and the fracture strain of the hydrogels obtained from the curves are listed in Fig. 6a.
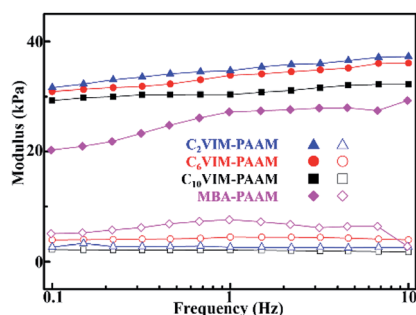

Fig. 5 The storage modulus (solid symbols) and loss modulus (open symbols) of the hydrogels at 25 °C obtained from DMA tests.
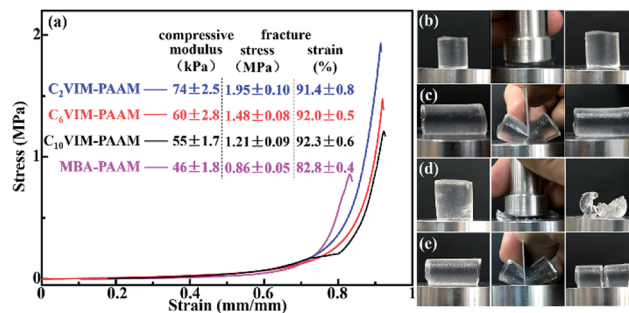

Fig. 6 (a) Compressive stress–strain curves of the hydrogels (inset is the compressive modulus, the fracture stress and the fracture strain of the hydrogels obtained from the curves); (b) and (c) images of the C_6VIM–PAAM hydrogel under compression and slicing with a blade, respectively; (d) and (e) images of the MBA–PAAM hydrogel under compression and slicing with a blade, respectively.

With the increasing in the length of the crosslinkers in C_nVIM–PAAM hydrogels, the compressive modulus and the fracture stress of C_nVIM–PAAM hydrogels decreased, but the fracture strain increased. The C_nVIM–PAAM hydrogel crosslinked by shorter crosslinker might formed more rigid network with a higher deformation resistance, which needed more stress to achieve compressive deformation. Correspondingly, the C_nVIM–PAAM hydrogel crosslinked by longer crosslinker might formed more flexible network to allow larger deformation. C_nVIM–PAAM hydrogels exhibited a better performance to withstand compressive stress and deformation compared with MBA–PAAM hydrogel, which indicated a more efficient energy dissipation in C_nVIM–PAAM. The mechanical strength of C_nVIM–PAAM hydrogels was also higher than that of the reported chemically crosslinked hydrogels.[24,25] C_nVIM–PAAM hydrogels also exhibited better performance to sustain slicing than MBA–PAAM hydrogel (Fig. 6c and e), and showed good and fast recoverability, which could recover its original shape immediately after the external force released (Fig. 6b and c).

3.4 Thermal stability

The thermal stability of the C_nVIM crosslinked networks was firstly characterized by TG analysis. All the freeze-dried C_nVIM–PAAM hydrogels exhibited a similar decomposition process. Take C_6VIM–PAAM as an example (shown in Fig. 7), the weight loss below 120 °C was ascribed to the dehydration. After dehydration, the weight loss followed a degradation mechanism with two major steps. The onset decomposition temperature of C_6VIM–PAAM was 263 °C. The first decomposition step of C_6VIM–PAAM occurred from 263 to 345 °C arose likely from the elimination of ammonia gas from amide groups of PAAM chains. The second decomposition step occurred from 330 to 500 °C, which was attributed to the decomposition of the polymer backbone and the cross-linked network structure.[26] MBA–PAAM hydrogels also decomposed in two steps similarly to C_6VIM–PAAM, but showed a relatively poor thermal stability of the polymer backbone than C_nVIM–PAAM hydrogels, as shown in Fig. 7.

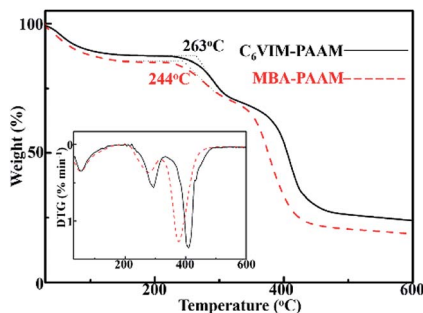The as-prepared hydrogels (35 mm in diameter and 40 mm in height) were further sealed in a stainless mold to perform

Fig. 7 TGA curves of the freeze-dried C_6VIM–PAAM and MBA–PAAM hydrogels (inset is the DTG curves of the hydrogels).
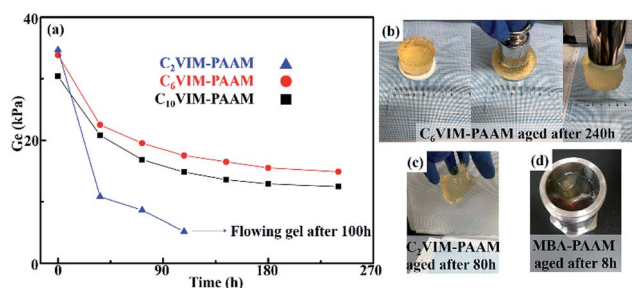

Fig. 8 (a) Plateau storage modulus of C_nVIM–PAAM hydrogels aged at 150 °C as a function of time; (b) images of C_6VIM–PAAM hydrogel aged at 150 °C for 240 h; (c) image of C_2VIM–PAAM hydrogel aged at 150 °C for 80 h; (d) images of MBA–PAAM hydrogels aged at 150 °C for 8 h.

aging test at 150 °C and the thermal stability of the hydrogel were determined by the remained storage modulus of the aged hydrogels, as shown in Fig. 8a. For all the C_nVIM–PAAM hydrogels, the modulus decreased sharply in the initial 80 h and the colorless hydrogels became slight yellow (Fig. 8b and c). C_6VIM–PAAM and C_{10}VIM–PAAM hydrogels showed excellent thermal stability during the aging tests. After being aged at 150 °C for 240 h, both the hydrogels could retain more than 40% the original modulus. The aged hydrogels remained stable in shape and could still withstand external force and compressive strain, as shown in Fig. 8b. However, C_2VIM–PAAM hydrogel consumed more than 80% the initial modulus, which lost its initial shape and became a flowing gel unable for further DMA tests after being aged for 100 h, as shown in Fig. 8c. Despite the relatively poor stability compared with C_6VIM–PAAM and C_{10}VIM–PAAM hydrogels, the thermal stability of C_2VIM–PAAM hydrogel was still much superior than that of MBA–PAAM hydrogel. MBA–PAAM hydrogel lost the hydrogel nature and became a liquid within 8 h after being aged at 150 °C, as shown in Fig. 8d. These results suggested that using C_nVIM as crosslinkers for PAAM hydrogel preparation greatly improved the thermal stability of the crosslinked networks.

4 Conclusions

A series of polyacrylamide hydrogel were prepared *via in situ* solution copolymerization using bis-vinylimidazolium bromides as crosslinkers. The bis-vinylimidazolium bromides

crosslinked networks showed good swelling degradation resistance with equilibrium water contents up to 75.9 g g^{-1}. The prepared hydrogels were mechanically strong under compression with a compress modulus higher than 55 kPa and a fracture stress higher than 1.2 MPa and a fracture deformation higher than 90% strain. More importantly, the hydrogels showed superior thermal stability, which could tolerate 150 °C for more than 240 h without fracture. Our work here shows the great potential of the bis-vinylimidazolium bromides as optional crosslinkers for PAAM hydrogels towards real world applications, such as water management in high-temperature petroleum reservoirs.

Conflicts of interest

There are no conflicts to declare.

Acknowledgements

Notes and references

1 K. Lee and D. Mooney, *Chem. Rev.*, 2001, **101**, 1869.
2 Y. Qiu and K. Park, *Adv. Drug Delivery Rev.*, 2001, **53**, 321.
3 M. Baker, S. Walsh, Z. Schwartz and B. Boyan, *J. Biomed. Mater. Res., Part B*, 2012, **100**, 1451.
4 J. Holtz and S. Asher, *Nature*, 1997, **389**, 829.
5 S. Basak, N. Nandi, S. Paul, I. W. Hamley and A. Banerjee, *Chem. Commun.*, 2017, **53**, 5910.
6 N. Nandi, K. Gayen, S. Ghosh, D. Bhunia, S. Kirkham, S. K. Sen, S. Ghosh, I. W. Hamley and A. Banerjee, *Biomacromolecules*, 2017, **18**, 3621.
7 D. Zhu, B. Bai and J. Hou, *Energy Fuels*, 2017, **31**, 13063.
8 H. Kamata, Y. Akagi, Y. Kayasuga-Kariya, U. Chung and T. Sakai, *Science*, 2014, **343**, 873.
9 E. Appel, J. Barrio, X. Loh and O. Scherman, *Chem. Soc. Rev.*, 2012, **41**, 6195.
10 T. Nakajima, T. Kurokawa, S. Ahmed, W. Wu and J. Gong, *Soft Matter*, 2013, **9**, 1955.
11 M. Caulfield, G. Qiao and D. Solomon, *Chem. Rev.*, 2002, **102**, 3067.
12 D. Zhu, J. Hou, X. Meng, Z. Zheng, Q. Wei, Y. Chen and B. Bai, *Energy Fuels*, 2017, **31**, 8120.
13 S. Zhang, J. Zhang, Y. Zhang and Y. Deng, *Chem. Rev.*, 2017, **117**, 6755.
14 M. Muldoon and C. Gordan, *J. Polym. Sci., Part A: Polym. Chem.*, 2004, **42**, 3865.
15 X. Zhang, X. Wang, L. Li, S. Zhang and R. Wu, *React. Funct. Polym.*, 2015, **87**, 15.
16 P. Kasák, J. Mosnáček, M. Danko, I. Krupa, G. Hloušková, D. Chorvát, M. Koukaki, S. Karamanou, A. Economou and I. Lacík, *RSC Adv.*, 2016, **6**, 83890.
17 L. Chiem, L. Huynh, J. Ralston and D. Beattie, *J. Colloid Interface Sci.*, 2006, **297**, 54.

18 N. Yuan, L. Xu, L. Zhang, H. Ye, J. Zhao, Z. Liu and J. Rong, *Mater. Sci. Eng., C*, 2016, **67**, 221.

19 M. Song, Y. Wang, B. Wang, X. Liang, Z. Chang, B. Li and S. Zhang, *ACS Appl. Mater. Interfaces*, 2018, **10**, 15021.

20 G. Song, Z. Zhao, X. Peng, C. He, R. Weiss and H. Wang, *Macromolecules*, 2016, **49**, 8265–8273.

21 Y. Ohsedo, M. Taniguchi, K. Saruhashi and H. Watanabe, *RSC Adv.*, 2015, **5**, 90010.

22 F. Selen, V. Can and G. Temel, *RSC Adv.*, 2016, **6**, 31692.

23 P. Tongwa, R. Nygaard and B. Bai, *J. Appl. Polym. Sci.*, 2013, 38258.

24 M. Hu, X. Gu, Y. Hu, T. Wang, J. Huang and C. Wang, *Macromolecules*, 2016, **49**, 3174.

25 M. Song, Y. Wang, B. Wang, X. Liang, Z. Chang, B. Li and S. Zhang, *ACS Appl. Mater. Interfaces*, 2018, **10**, 15021.

26 R. Zolfaghari, A. Katbab, J. Nabavizadeh, R. Tabasi and M. Nejad, *J. Appl. Polym. Sci.*, 2006, **100**, 2096.